A methodology for processing raw LiDAR data to support urban flood modelling framework

A. F. Abdullah, Z. Vojinovic, R. K. Price and N. A. A. Aziz

ABSTRACT

An assessment has been carried out to study the performance of seven different LiDAR filtering algorithms and to evaluate their suitability for urban flood modelling applications. It was found that none of these algorithms can be regarded as fully suitable to support such work in its present form. The paper presents the augmentation of an existing Progressive Morphological filtering algorithm for processing raw LiDAR data to support a 1D/2D urban flood modelling framework. The existing progressive morphological filtering algorithm was modified to incorporate buildings with basement, passage buildings and solid buildings and its value was demonstrated on a case study from Kuala Lumpur, Malaysia. The model results were analysed and compared against recorded data in terms of flood depths, flood extents and flood velocities. The difference in flood depths of approximately 40% was observed between a model that uses a DTM modified by the progressive morphological filtering algorithm and the predictions of other models. The overall results suggest that incorporation of building basements within the DTM can lead to a significant difference in the model results with a tendency towards overestimation for those models which do not incorporate such a feature.

Key words | digital terrain models, LiDAR filtering algorithms, urban features, urban flood modelling

A. F. Abdullah (corresponding author)
Z. Vojinovic
R. K. Price
Department of Hydroinformatics and Knowledge Management,
UNESCO-IHE,
Westvest 72611 AX Delft,
Netherlands
E-mail: *abdul42@unesco-ihe.org*

N. A. A. Aziz
No 22 and 24, Jalan Wangsa Delima 6,
KLSC, Seksyen 5,
Pusat Bandar Wangsa Maju,
53300 Kuala Lumpur,
Malaysia

INTRODUCTION

In the last few decades the consequences of floods and flash floods in many parts of the world have been devastating with extensive tangible damages and unprecedented losses, personal pain, and social disruption. One way of improving flood management practice is to invest in data collection and modelling activities which enable an understanding of the functioning of a system and the selection of optimal mitigation measures. In this respect, the application of hydroinformatics technologies to urban water systems (the domain of urban hydroinformatics) plays a vital role in making the best use of the latest data acquisition and handling techniques coupled with sophisticated modelling tools, including uncertainty analysis and optimisation facilities to provide support to stakeholders for decision making (Price & Vojinovic 2011). These technologies have revolutionized the way in which communication of information is carried out, with large amounts of data and information stored at nodes (servers) and accessible to anybody with a computer or mobile phone connected to the Internet anywhere in the world (see also Abbot & Vojinovic 2009).

Some of the practical applications (or problems) where the use of urban hydroinformatics technologies plays critical role are: general system's performance evaluation, leakage control in water distribution networks, rehabilitation of sewerage networks, flood risk mitigation, analysis of treatment works operation, and minimising the impact of sewerage overflows on receiving waters. Since the safe and reliable models of urban water systems for operation and management are of increasing importance in both developed and developing countries, and since the systems are becoming more and more complex, there is a growing need to treat them in an integrated manner for which again the support of hydroinformatics tools is invaluable. There are many

doi: 10.2166/hydro.2011.089

examples which demonstrate the necessity of applying such tools for the management of urban water systems. For example, an application of urban hydroinformatics to flood management and disaster risk mitigation with the particular reference to the case of Dhaka City (Bangladesh) is given in Mynett & Vojinovic (2009). Dawson *et al*. (2008) have shown how the risk attribution can be used for a number of integrated urban flood risk management purposes including risk ownership, estimation of capacity to reduce risk and asset management.

Within the flood management process, data acquisition refers to the compilation of existing data and the collection of additional data for system analysis, modelling and decision making. A typical flood management database consists of spatial, temporal and other data (e.g. design standards, flood incidents, public perception of utility's levels of service, etc.). The collection of such data is of the utmost importance for making cost-effective investment and operational or maintenance decisions.

A digital terrain model (DTM) is one of the most essential items of information that flood managers need in present day practice. A DTM is essentially a topographic map that includes spot elevations for the terrain and data for its properties. Correspondingly, the term DEM (or digital elevation model), although usually associated with the land surface, refers to the elevations of any surface for any object. In urban flood management, DTMs are needed for an analysis of the terrain topography, for setting up 2D models, processing model results, delineation of flood hazards, production of flood maps, estimation of damages, and evaluation of various mitigation measures. Typically, a DTM data set can be obtained from ground surveys (e.g. total stations together with Global Positioning System – GPS), aerial stereo photography, satellite stereo imagery, airborne laser scanning or by digitising points/contours from an analogue format such as a paper map, so that they can be stored and displayed within a GIS package and then interpolated.

Airborne laser scanning (ALS) or light detection and Ranging (LiDAR) is one of the most common techniques that is used to measure the elevation of an area accurately and economical in the context of cost/benefit analysis. It can deliver information on terrain levels to a desired resolution. The end result of an ALS survey is a large number of spot elevations which need careful processing. In this research, the LiDAR System used was Riegl LMS Q560 with Full Waveform Analysis for unlimited target echoes. The pulse rate was 75 kHz or 75,000 points per second. This system used all echoes and all intensities. The beam size was less than 1.5 m diameter with 60 degrees swath width. The data has 40% side lap where the laser distance is approximately 700 m. The flying height was approximately 700 m above ground level with the average of 100 knots flying speed. The platform for this system was helicopter (Bell 206b JetRanger). This paper explores the use of different filtering algorithms and their value in processing LiDAR data so that it can be used more reliably in urban flood modelling applications.

In general terms, most existing filtering algorithms can be categorised into four groups. The first group of algorithms is based on mathematical morphological filtering. Vosselman (2000) proposed such filtering, which is closely related to the erosion operator used in mathematical morphology. The height difference between two adjacent points is used to determine the optimal filtering function that preserves the terrain features.

The second group can be described as progressive filters. In these filters some of the bare earth points are identified first and these are used to construct an initial triangulated irregular network (TIN). More terrain points are identified based on this TIN and are added to classify further points (Axelsson 1999). A sparse TIN is derived from neighbourhood minima, and then progressively made more dense. At every iteration a point is contrasted with the TIN. If it meets a certain criterion, it is added to the TIN. At the end of each iteration the TIN and the criterion are recomputed. The iterative process ends when there are no further points that conform to the criterion.

The third group of algorithms includes those that progressively increase the density of the points for the DTM in order to approximate the bare earth (see, for example, Elmqvist 2002). The ground surface is determined by employing an active shape model. A deformable model is used to fit the bare earth by means of progressively minimising the energy associated with the active shape model. When applied to LiDAR data, the active shape model behaves like a membrane floating up from underneath the data points. The manner in which the

membrane sticks to the data points is determined by an energy function. For the membrane to stick to the ground points, it has to be chosen in such a way that the energy function is minimized. Hu (2003), Wack & Wimmer (2002) and Pfeifer & Stadler (2001) used a hierarchical approach, which is similar to the image pyramid method used by Adelson *et al.* (1984). In that approach, a coarse DTM used is generated at the top level first and then it is refined hierarchically.

The fourth group of algorithms are filters based on segments. Points are segmented using cluster analysis, region growth or edge detection techniques based on height, normal curvature, slope or gradient differences within a small neighbourhood. The segments are then classified according to their contextual information (see for example, Sithole & Vosselman 2004).

URBAN FLOOD MODELLING PRACTICE

Traditionally, one-dimensional (1D) hydrodynamic models are used as standard for flood modelling. The 1D Saint-Venant equations for the conservation of mass (continuity) and momentum, typically with averaged cross-sections, are used to describe the evolution of the water depth h and either the discharge Q or the mean flow velocity V. The boundary conditions are either discharges or water levels (or the equivalent depths) at the two ends of the conduit or channel. For a channel network, the boundary conditions internally are not known in advance and therefore they are determined by the numerical solution procedure. The solution is commonly based on a temporary elimination of variables at internal cross-sections and a reduction of the equations to a system of unknown water levels at the nodes of the network.

Where flood flows are confined to well-defined conduits, a robust 1D model can be found sufficient. However, the flows generated along urban floodplains are normally highly complex because of the complicated morphology of the urban surface, and flows may run contrary to natural flow paths. The modelling of flows in such complicated geometrical situations is difficult and usually necessitates the coupling of 1D and 2D models; see, for example, Hsu *et al.* (2000), Mark *et al.* (2004), Djordjevic *et al.* (2005), Chen *et al.* (2006), Vojinovic *et al.* (2006), and Vojinovic & Tutulic (2009). The coupling of 1D and 2D models can also be done using OpenMI. The OpenMI standard defines an interface that allows time dependent models to exchange data at runtime. Model components that comply with the OpenMI standard can, without any programming, be coupled to OpenMI modelling systems (Becker & Schuttrumpf 2010). The system of 2D shallow water equations consists of three equations: a continuity equation and two equations for the conservation of momentum (in Cartesian coordinates). The numerical models for the shallow water equations are often based on the alternating direction implicit (ADI) two-step algorithm using a staggered C-grid system (see Hunter *et al.* 2008). An efficient solution consists basically of consecutive line sweeps across the domain (Petersen *et al.* 2007). and is reasonably robust and accurate (Abbott & Rasmussen 1977). The ADI algorithm implies that super-critical flow has to be approximated, but this does not result in a significant decrease in global accuracy of the solution.

For an efficient use of 2D models the collection and processing of terrain data is of vital importance. Typically, ALS surveys enable the capture of spot heights at a spacing of 0.5 m to 5 m with a horizontal accuracy of 0.3 m and vertical accuracy of 0.15 m. Most ALS surveys result in a substantial amount of data which require careful processing before they can be used for any application. Recently, the vertical accuracy of LiDAR has increased dramatically to 0.05 m. This extremely high resolution data brings considerable benefits but implies that data storage increases considerably and leads to more problems especially in hardware capability and the time taken for processing and modelling. In order to estimate the inundation flow in a populated area accurately detailed land features must be modelled properly, especially in resolving the dynamic processes of inundation. A precise, rational and efficient treatment of geospatial information is essential for practical use (Tsubaki & Fujita 2010). Typically, thinning, filtering and interpolation are techniques that need to be adopted as part of this process. Thinning (or reduction of data points) is usually achieved by removing neighbouring points that are found to be within a specified elevation tolerance. Filtering is a process of automatic detection and interpretation of bare earth and

objects. To date, many filtering algorithms have been developed but none of them can be considered as fully suitable for the needs of urban flood modelling. The following section discusses issues concerning the use of spatial data for urban flood modelling.

ISSUES CONCERNING SPATIAL DATA

Urban features

Urban environments can contain a vast variety of features (or objects) that have a role in storing and diverting flows during flood events. In this respect, buildings are the most significant objects, and in broad terms they can be divided into three types: buildings with basements, passage buildings, and buildings which have neither basements nor passages; see Figure 1. Typical examples of buildings with basements are those that have underground car parks that can be filled with water during flood events. Passage buildings refer to those that have no basements but which have large open spaces and corridors that can allow flow through the site. The third category refers to those buildings that can act as solid objects and can fully divert any floodwater. In addition to buildings, there are also many small geometric 'discontinuities' such as roads, stairs, pavement curbs, fences and other objects which can play an important role in diverting flows that are generated over the urban surface. These features can be undetected by airborne LiDAR but would probably be detected by mobile terrestrial LiDAR (Roncat *et al.* 2010). When these features are not adequately represented it is highly likely that the flood model will not be able to produce satisfactory results.

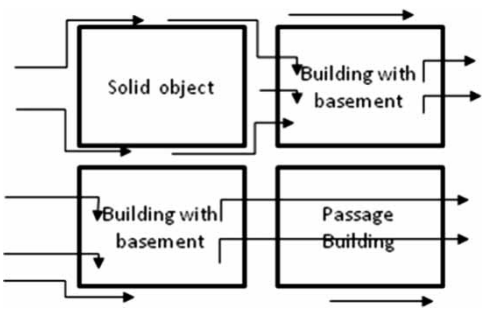

Figure 1 | Schematisation of the water flow through and around different types of buildings.

DTM resolution

In terms of the DTM resolution, it is clear that a higher resolution 2D will capture urban features better whereas such features would be smeared or completely removed when the grid is coarsened. An illustration of the effect on buildings and roads of increasing the 2D model grid size is given in Figure 2.

Furthermore, research to date shows that 2D models derived from a coarser DTM resolution tend to generate a more widespread distribution of flood water with shallower depths compared with those models based on a finer DTM resolution. In the case of the finer resolution model the flood water tends to get trapped by local terrain depressions and thus generates larger depths (Vojinovic *et al.* 2010b); see example given in Figure 3.

It is important to note that present computing resources still impose a challenge for modelling the terrain of large scale areas, in which case increasing the grid size can effectively improve efficiency, but it can also cause a significant reduction in detail. Again, the straightforward 2D flow modelling technique may not reflect properly the local flow phenomena in coarse grid applications. In such a case an approach based on the

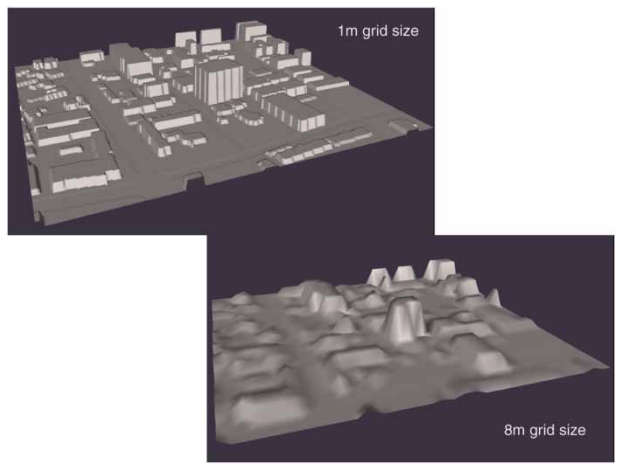

Figure 2 | Effects of grid resolution on capturing building and road features (*Source:* Vojinovic & Abbott 2011).

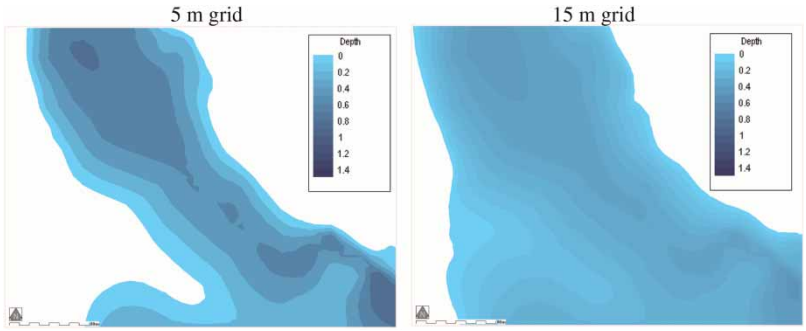

Figure 3 | Example of computed water depths for 5 m (left) and 15 m (right) DTM resolution using 2D (MIKE21) model (see also Vojinovic *et al*. 2010a).

adjusted conveyance and storage characteristics may prove beneficial (see for example, Seyoum *et al*. 2010; Vojinovic *et al*. 2010a). Furthermore, parallel computing is worthwhile exploring; see for example Neal *et al*. (2009, 2010). Also, Lamb *et al*. (2009) demonstrated that the use of technology from the computer graphics industry to accelerate a 2D diffusion wave (non-inertial) floodplain model can be found beneficial.

Filtering algorithms

As LiDAR has increased our capabilities to obtain high resolution data, the processing of such data is still a challenging job. The tasks in LiDAR data processing include the 'modelling of systematic errors', 'filtering', 'feature detection' and 'thinning'. Of these tasks, filtering and quality control pose the greatest challenges, consuming an estimated 60% to 80% of the processing time and thus underlining the necessity for on-going research in this area (Schumann *et al*. 2007).

The first pulse is used for DTM generation. The generation of a DTM involves the identification of bare earth points, and the removal of non-terrain points such as vegetation, buildings and other objects. The process of removing points, or finding a ground surface from a mixture of ground and vegetation measurements, is referred to as filtering and classification. To date, a number of filtering and classification algorithms have been developed. Some of these algorithms have been published while others are not known in detail because of proprietary restrictions. The following sections describe some existing filter algorithms and the improvement of one of these algorithms for better urban flood modelling.

OVERVIEW OF EXISTING LIDAR FILTERING ALGORITHMS

Seven different filtering algorithms from the different groups referred to above are considered. They are: two morphological algorithms (first group), a TIN-based algorithm (second group) and four shape-based algorithms (third group). These seven algorithms are the algorithms most widely used by researchers as well as industry practitioners.

Progressive morphological filter (1D and 2D)

The main assumption of this algorithm is that points in a given height range within a neighbouring measurement point are for bare earth. In the 1D progressive morphological algorithm the lowest point in a neighbourhood is labelled as a terrain point. By gradually increasing the window size and using elevation difference thresholds, it removes measurements for different sized non-ground objects while preserving ground data. The maximum elevation difference threshold can be set either to a fixed value to ensure the removal of large and low buildings in an urban area or to the largest elevation difference in a particular area. The filtering window can be a one-dimensional line or a two-dimensional rectangle or any other shape. When a line window is used, the opening operation is applied to both x and y directions at each step to ensure that the non-ground objects are removed (Zhang *et al*. 2003).

Two fundamental operations in this algorithm are *dilation* and *erosion*. These operations are commonly employed to enlarge or to reduce the size of features.

These concepts can also be extended to the analysis of a continuous surface such as a digital surface model as measured by LiDAR data. For a LiDAR measurement $p(x, y, z)$ the dilation of elevation z at x and y is defined as

$$d_p = \max_{(x_p, y_p) \in w} (z_p) \quad (1)$$

where d_p is the dilation of elevation, p is the point cloud, x_p is the x coordinate of the point, y_p is the y coordinate of the point, z_p is the height value of the point and w is the window.

Erosion is a counterpart of dilation and it is defined as

$$e_p = \min_{(x_p, y_p) \in w} (z_p) \quad (2)$$

where e_p is the erosion of elevation.

The combination of erosion and dilation generates opening and closing operations that can be used to filter the LiDAR data. An erosion of the data set followed by dilation is performed to generate the opening operation, while the closing operation is accomplished by carrying out dilation first and then erosion. An erosion operation can remove tree objects of sizes smaller than the window size. Dilation can be used to restore the shapes of large building objects. The ability of an opening operation to preserve features larger than the window size is very useful in some applications (see also Zhang *et al.* 2003). For example, the measurements of large buildings can be preserved if the morphological filters are applied to the LiDAR measurements for a dense urban area. The schematic of the algorithm is given in Figure 4.

The 2D progressive morphological algorithm adopts the same concept, the only difference is that the filtering window has a two-dimensional rectangle or any other shape. Apart from using the line, it also uses a square window which can perform erosion in the x direction first and then in the y direction. The same rule can be applied to dilation. The weakness of this filter is that the result is influenced by the final window size and the final threshold value for which the points are expected to be terrain points. Too small a window leads to large building points labelled as ground points. Too high a threshold leads to many vegetation points labelled as ground points. The strength of this filter is that the entire process is carried out by gradually increasing the window size, and it can be controlled by the user.

This algorithm has the ability to remove non-ground objects, such as buildings and trees, with typical processes including opening, closing, dilatation and erosion based on kernel operators. When applied to urban flood modelling, this research has shown that the algorithm has good filtering capabilities of unwanted objects such as vegetation and cars. However, the same algorithm can also filter out all buildings, which cannot be regarded as a positive because the buildings are very much needed for flood modelling.

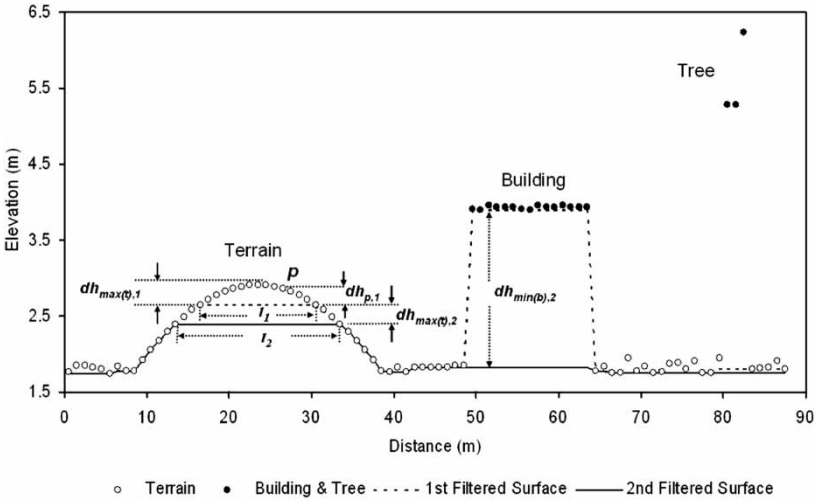

Figure 4 | Schematics of the morphological filter for separation between ground and non-ground measurement (Zhang *et al.* 2003).

Elevation threshold with expand window (ETEW) filter

The main assumption of this algorithm is that the elevation changes of neighbouring measurement points are distinct between ground, trees and buildings in a limited size area within a search window (Zhang & Whitman 2005). Elevation differences in a certain area are used by the algorithm to separate ground and non-ground LiDAR measurements. The non-ground points are identified and removed by the elevation threshold method using an expanding search window. The weakness of this filter is that it is unable to find the right elevation threshold value. Its strength is that the inherent concept and calculation are rather simple and straightforward.

The ETEW filter can sometimes create abrupt elevation changes of preserved ground measurements near cell boundaries because minimum elevation thresholds are different for each cell. Usually, the elevation threshold value will cause the buildings and vegetation points to be labelled as ground points and included in the DTM. This situation makes this filter able to preserve the buildings and vegetation in a complex urban environment. Since the buildings and vegetation represent important features in an urban area, their preservation without proper handling may have a considerable impact on the floodwater flow. Furthermore, in relation to urban flood modelling, this algorithm has not performed well in that it produces far too much noise in the resulting DTM. Even though the buildings are not filtered out as is the case with the previous algorithm, the buildings can only be represented as solid objects.

Maximum local slope filter

The main assumption of this algorithm is that the terrain slopes are different from the slope that can be found between the ground and the top of a building. In this algorithm, a comparison of the local slopes between the LiDAR point and its neighbourhood are used to identify point measurements. These slopes are used to separate the ground from non-ground points. It is assumed that along the boundaries of the ground and non-ground areas, the slopes between the ground and its neighbouring non-ground points are much larger than those between the ground and its neighbouring ground points. This filter uses the slope of the line between any two points in a point set as the criterion for classifying ground points. The technique relies on the premise that the gradient of the natural slope of the terrain is distinctly different from the slopes of non-terrain objects (trees, buildings, etc.). Any feature in the laser data that has slopes with gradients larger than a certain predefined threshold is classified as a point that does not belong to the natural terrain surface (Sithole & Vosselman 2001). The weakness of this filter is that it is vulnerable to slope change. When applied to steep slopes, the filter usually fails to extract the ground points. The strength of the filter is that it can detect high structures such as tall buildings which are often found in many urban environments.

This filter preserves a better shape of the ground objects as it is sensitive to small, sharp changes in area, such as for shrubs, and short walls, which are difficult for most filters. This is because a point is classified as a ground point if the maximum slope of the vectors connecting the point to all its defined neighbours does not exceed the maximum slope within the study area, which in an urban environment may be very large due to the high elevation buildings. As a result, the final DTM will have too many unwanted objects such as trees, cars, etc.

Iterative polynomial fitting

The assumption of this algorithm is that the lowest point in a set of neighbouring measurement points belongs to the ground. In this algorithm, LiDAR points are classified by selecting ground measurements iteratively from the original data set. The lowest point within a large moving window (which is usually larger than the non-ground object in a particular area) consists of an initial set of ground measurements. For example, ground measurements at the top of a small mountain can be missed because the interpolated surface is too low due to lack of previously identified ground points at the mountain top (Zhang & Cui 2007). This error can be recovered by comparing the elevation difference of a candidate ground point to the current surface. When compared with current surface, the points at the top of a mountain will be identified as ground measurements because their elevation differences from current surface are less than a predefined threshold. However, other non-

ground points might be included mistakenly. To remove these errors, the fitness of the previous and current surfaces to ground measurements within a surface interpolation window needs to be introduced as another criterion. If the fitness of the current surface is better than the previous one then the missed ground point is recovered. The weakness of this filter is that its result tends to have a lower value than the real data. Overall, this algorithm has the tendency to produce misleading information and if the final DTM is directly used for modelling of urban floodplains, without post-processing, it will certainly have negative consequences.

Polynomial two surface filter

The main assumption of this algorithm is that the ground is essentially represented as being continuous or at least a piecewise continuous surface. A polynomial 2-surface filter uses a mathematical function to approximate the ground. A least squares adjustment is used to detect the non-ground points as if they were incorrect by reducing their weights in each iteration calculation (Zhang & Cui 2007). This method usually requires flat areas and does not work well in a mountainous terrain or where the buildings appear more like hills. With this method only small objects and the boundaries of larger elements can be eliminated because the edges of very high buildings cannot be detected due to the resolution failure and thresholds. This is because points within a certain vertical distance above the surface are treated as ground points. If used in urban flood modelling work, the high buildings and elevated structures such as elevated roads and flyovers that are included will create artificial obstacles to the flow. This algorithm also has a tendency to produce too much noise in the resulting DTM which makes it inappropriate for urban flood modelling applications.

Adaptive TIN filter

The main assumption of this algorithm is that nearby points have similar attributes while distant points have dissimilar attributes. In this algorithm, the distance of point on the surface of a TIN is used to select ground points from a LiDAR data set. A sparse TIN is derived from neighbourhood minima, and then progressively made more dense depending on the laser data. In an iteration a point is added to the TIN if the point meets certain criteria in relation to the triangle that contains it. The criteria are that the angle a point makes to the triangle must be below a certain threshold and a point must be within the minimum distance of the nearest triangle node. At the end of an iteration, the TIN and the data-derived thresholds are recomputed. New thresholds are computed based on the median values estimated from the histograms at an iteration. Histograms are derived for the angle points to generate TIN facets and the distance to the facet nodes. The iterative process ends when there are no points that are below the threshold (Axelsson 1999). The weakness of this algorithm is that it needs large data storage and significant computational time for execution. This algorithm can successfully remove small buildings and most bridges, but it will fail to remove some larger buildings. This is because the algorithm uses a fixed window size to calculate the mean values and it will fail to remove those objects that are larger than the window size. If the resulting DTM is used for urban floodplain modelling then the results are likely to be erroneous in those areas where such buildings exist.

Evaluation of algorithms

A qualitative assessment was undertaken to evaluate all of the algorithms mentioned above. In this assessment, criteria were used that focus on the removal of buildings, flyovers and bridges and the capture of curbs and river alignment. The assessment was done by visually assessing the performance and giving a mark with a weighted value. This weighted value is based on the filter performance in removing and capturing the features. If more than 75% of the features are removed or captured the filter is given 1 mark; if 50% to 75% of the features are removed or captured the filter is given 2 marks; if 25% to 50% of the features are removed or captured the filter is given 3 marks and if less than 25% of the features are removed or captured the filter is given 4 marks. The least total mark will suggest which filter performs the best based on the selected criteria. The results show that each filter acts differently and has different features depending on its filtering concept. The summary of the evaluation is given in Table 1. From Table 1 it can be observed that the Morph algorithm performs well in removing bridges, buildings, vegetations and flyovers. Since the Morph2D algorithm uses similar concept

Table 1 | Summary of qualitative assessment

Indicator	Morph	Morph2D	ETEW	Slope	Polynomial	Poly2surf	ATIN
Building removal	2	2	4	4	4	3	3
Bridge removal	2	4	3	4	3	4	3
Flyover removal	2	1	4	3	1	3	2
Curbs capturing	1	2	1	2	2	2	3
River alignment	2	3	3	2	3	2	2
Vegetation removal	1	2	3	3	1	4	1
Total weighted value	10	14	18	18	14	18	12

Weighted value: 1 = Excellent, 2 = Fair, 3 = Acceptable, 4 = Poor.

to Morph algorithm its results are close to Morph: the only difference is observed with respect to the handling of bridges.

In an urban environment the difference between the ground points and the top of buildings are so big, some of the filters perform ineffectively. Because the ETW filter is not iterative, the determination of the threshold in a big difference in height leads to buildings and flyovers being captured while less points are removed. In the Slope filter, a big difference in height produces a steep slope and leads to a large gradient being predefined as the threshold. This situation leads to most of the points being preserved and the removal of points being minimised. With poly2surf most of points are classed as ground points. Therefore this algorithm performs well in capturing buildings and curbs but is less efficient in removing bridges, flyovers and vegetation.

The Polynomial filter results show a good capability in removing features. This is because most of the elevated feature points are missed due to the lowered interpolated surface, which results from the lack of previously identified ground points in the elevated area. As for the ATIN algorithm most objects smaller than the window size, including buildings and flyovers, are removed successfully. Most of the bridges located near bare earth failed to be removed.

All filters give acceptable results for curbs and river alignments. Morph appears to have the least overall total mark. This suggests a better performance in developing the urban DTM that is required as input for the urban flood model. Supported by this qualitative assessment result, the Morph filter is regarded as the basis for modifying LiDAR data in order to deduce the urban DTM needed for flood modelling.

MODIFICATION OF THE PROGRESIVE MORPHOLOGICAL ALGORITHM (MPMA)

As indicated above, out of the seven algorithms reviewed in this paper the progressive morphological algorithm (PMA) has been shown to be more promising than the other algorithms and as such it was selected for further development. This is mainly due to its strength in separating ground and non-ground points by increasing the window size iteratively. In particular, the algorithm gives the possibility that the user can be in control while removing and preserving objects. The code of this improved algorithm was written in Visual Basic. The objectives of the improvement work are focused on the following issues:

- to detect buildings and to classify them into: solid buildings, passage buildings and buildings with basements;
- to remove simple bridges along a river;
- to detect flyovers and light train lines, to remove related objects and to reconstruct structures that are underneath;
- to retain curbs;
- to detect riverbanks and to interpolate points between the banks where the river network is modelled with a 1D model (MIKE11), and to generate a DTM for use with a 2D model (MIKE21);
- to test the usefulness of the algorithm by carrying out the 1D/2D modelling work for a study area.

In order to fulfil the filtering algorithm objectives, the development process is divided into four major parts. Each part is concerned with one of the selected essential

objects in urban environment namely buildings, bridges and flyovers, curbs and river channel. The overall flowchart for this new filtering algorithm is shown in Figure 5.

The detection and classification of buildings was carried out as a three step procedure:

Step 1: detect buildings from point cloud data;
Step 2: separate objects from point cloud data;
Step 3: classify building.

Detection of buildings from point cloud data

In this step, the existing morphological algorithm is improved by initially detecting and labelling all the

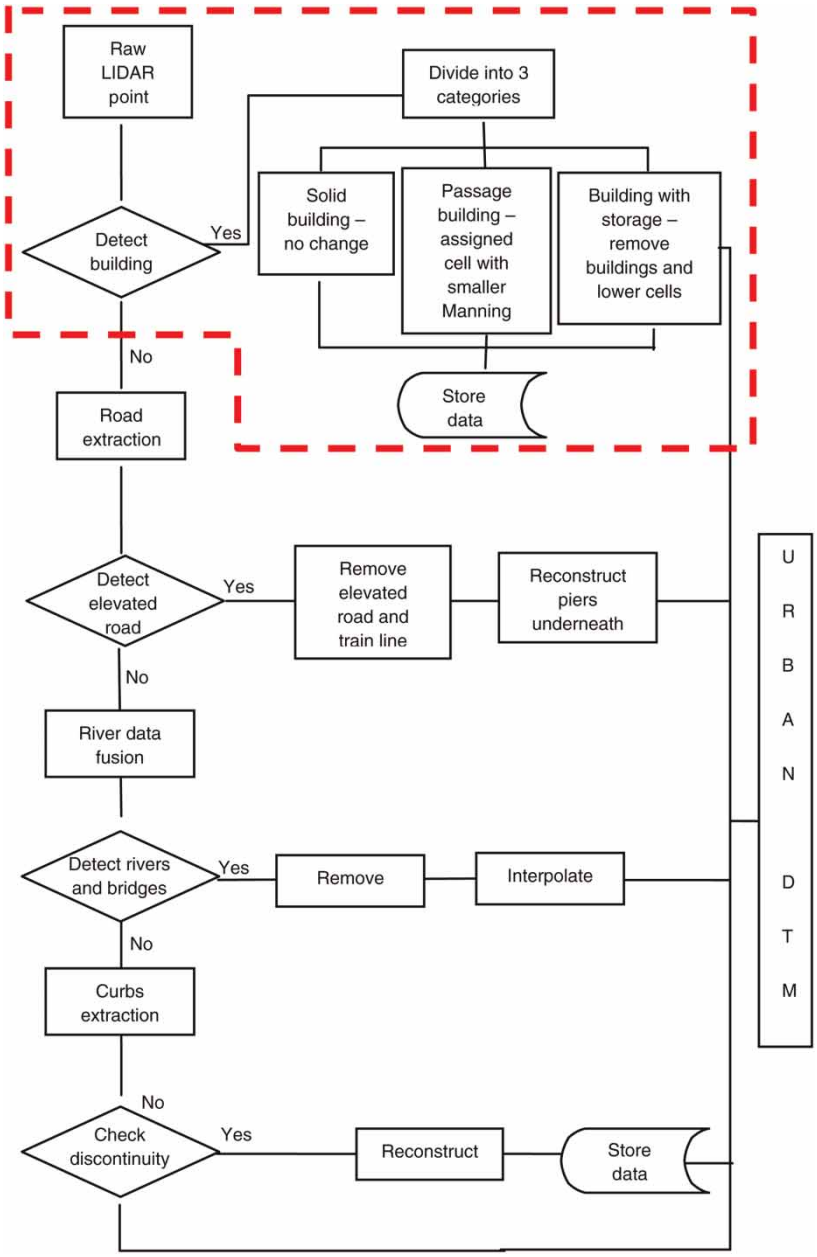

Figure 5 | Flowchart for the development of the new filtering algorithm.

buildings. This process is done by manipulating the slope concept. It is based on the following assumptions:

1. terrain slopes are different from the slopes that are found between the ground and the top of a building;
2. buildings are highly elevated objects in an urban area;
3. most buildings in an urban area have smoothly sloped roofs.

Initially, points are labelled as 'High' or 'Low' based on their elevation. In the present development, the value for 'High' points was left to be user-defined. Then, for each point in point cloud, the slope in percentage rise is calculated for a 3×3 neighbourhoods around every point (Figure 6, right). The maximum value of the slope from these neighbourhoods is taken as an attribute for that point (see Figure 6, left).

Based on the slope, points are divided into two classes; 'Steep' and 'Slight'. The initial slope is user-defined and is usually the slope between the building which has a, minimum value of height, and the surface. The members of the Steep class are those points representing vegetation and walls of buildings, while the members of the Slight class are the representatives of building roofs and relatively flat areas on the surface. Points that represent a building wall are points with a 'High and Steep' label. These points are selected and converted to a vector form as polygons. Based on the assumption that a building should lead to the creation of a closed polygon in vector form, all created polygons are tested if they are closed or not. Points that do not create closed polygons are usually represented as high land and vegetation. These unclosed polygons are then removed. The closed polygons are converted back to raster form as a grid.

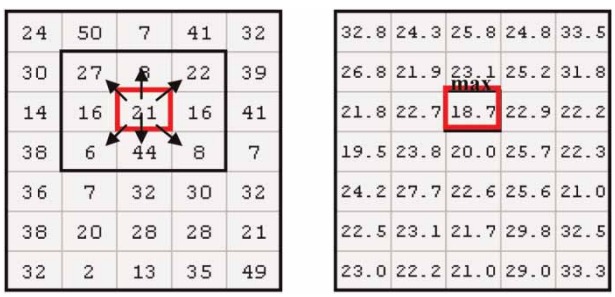

Figure 6 | The concept of the slope calculation.

Separation of other objects from point cloud data

The purpose of this is to remove the vegetation and other objects from point cloud data. The procedure is based on the original progressive morphological algorithm. Apart from the advantage for the user in controlling the separation of ground and non-ground points, this algorithm is also found to be useful because of its relatively simple structure as well as its effectiveness in separating ground and non-ground points.

Classification of building objects

In this step, the original morphological filtering algorithm was improved by assigning the buildings that have been preserved with the three types of properties namely; buildings with basement, passage buildings and solid objects. For points detected as buildings with basement, the point elevation was changed by lowering it to a certain depth below the ground surface depending on the number of basement levels. In this case, a place for the retention of flood water is created. The determination of depth is dependent on the characteristics of the study area. The examples of such characteristics are the average height of ground surface, the elevation of the highest building and the basement height. In this algorithm, these characteristic are defined by the user based on the study area. If no information is input for these characteristics, standard values are used. Points with a passage building label have an elevation value that is similar to the average ground surface. This point is then assigned a Manning value (roughness parameter) of 20 ($n = 0.05$) while the rest is assigned a Manning value of 30 ($n = 0.033$) and exported as an ASCII file. Smaller Manning values lead to the flow having some resistance when passing through the passage building pixel. The determination of the Manning value is explained in the Case Study section. This ASCII file is used to generate the dfs2 file (grid file in MIKE21) which is used later in flood modelling. For solid building points, the original elevation is kept. When this process is done, points are merged back with the pre-DTM points.

CASE STUDY

The study area concerns a small part of the Klang River basin. It is located on the west coast of Peninsular Malaysia in

Federal Territory of Kuala Lumpur. The Klang River basin is the most densely populated area of the country with an estimated population of over 3.6 million and growing at almost 5% a year. Although the major flood mitigation works within the Kuala Lumpur city have, to a large extent, been implemented, flooding in the city is still frequent and severe. This is causing disruption to various activities in the city as well as extensive flood losses suffered by the flood victims.

Urbanisation and industrialisation in the river basin have been rapid with major portions of agricultural and ex-mining land being converted for urban use. It is estimated that about 50% of the Klang River Basin has been developed for residential, commercial, industrial and institutional use. As a result of the extensive and rapid urban development in the basin area, problems emerged in the form of river overbank floods, flash floods that afflict clogged drainage systems and river environment degeneration. This prompted the commissioning of a number of flood mitigation and river environment enhancement programmes as the problems and the associated social and economic costs were escalating with further urbanization. The Government of Malaysia, through the department of irrigation and drainage (DID) as its implementing agency, now intends to approach the problems more holistically through the integrated river basin management (IRBM) approach to improve the river environment and flood mitigation works in the Klang River Basin. A field survey has been carried out in order to classify the buildings into those that have basements, passage buildings and those that can be regarded as solid objects. Out of 191 surveyed buildings 51% were found to be the buildings with basements, 43% passage buildings and 6% solid object buildings (see Figure 7).

The analysis of survey data indicates:

- 92% of buildings which have a height in the excess of 20 metres have basements;
- 85% of buildings which have a height between 5 to 20 metres have a significant open space on the ground floor;
- 87% of solid objects which are less than five metres high have neither basements nor open space on the ground floor.

For buildings with basement, the average basement depth found was in the order of five metres. The values gathered from this survey are used to define the characteristics of study area.

Modelling framework

The model of the study area contains the river network and urban floodplains for which the 1D/2D commercial software packages MIKE11/MIKE21 (i.e. MIKEFLOOD) were utilised. The MIKE 11 model of the river was developed and calibrated previously by DHI (2004). For the purpose of comparing different LiDAR filtering algorithms five

Figure 7 | Example of a building with basement (left), a solid object building (top right corner) and a passage building (bottom right corner).

2D models were generated from 1-metre grid DTMs. The DTMs were generated from the Morph, Morph2D, Poly, ATIN and MPMA algorithms. From the comparison of the DTMs it can be observed that only the MPMA algorithm has the ability to incorporate buildings according to their characteristics; see Figure 8.

The setting of the Manning's roughness coefficients for flood plains follows the standard settings for MIKE 21. A Manning number (m) of 30 ($n = 0.033$) was found to be a practical starting value in most floodplain applications. By altering Cowan's (1956) procedure which was developed for estimating n values for channels, the following equation can be used to estimate n values for a flood plain (Arcement & Schneider 1984):

$$n = (n_b + n_1 + n_2 + n_3 + {}_4)m \tag{3}$$

where n_b is a base value of n for the flood plain's natural bare soil surface, n_1 is a correction factor for the effect of surface irregularities on the flood plain, n_2 is a value for variations in shape and size of the flood-plain cross section, assumed to equal 0.0, n_3 is a value for obstructions on the flood plain, n_4 is a value for vegetation on the flood plain and m is a correction factor for sinuosity of the flood plain, equal to 1.0 in this study.

The values for n_b, n_1, n_2, n_3, n_4 and m can be determined from Table 2.

In this research, the Manning value adopted for MIKE21 model is 30 ($n = 0.033$) for the entire surface except for the cells that represent passage buildings. The Manning value of 20 ($n = 0.05$) is used for a passage building, to emulate disturbances due to local obstacles (shops, bike racks, etc.). This value is determined from Equation (4):

$$\begin{aligned} n &= (n_b + n_1 + n_2 + n_3 + n_4)m \\ n &= (0.03 + 0.00 + 0.006 + 0.004 + 0.01)1 \\ n &= 0.05 \end{aligned} \tag{4}$$

The coupled 1D/2D models simulate the flow in the Klang River and tributaries and the overtopping of flow along the streets of Kuala Lumpur.

Discussion of model results

The models were simulated using two historical rainfall events (29 October 2001 and 10 June 2003) that caused severe floods within the study area. The model results were analysed in terms of flood depths and extent of flooded area and compared against the recorded data from several locations. The data was obtained from drainage and irrigation department of Malaysia (DID). The rainfall data used in model simulations was gathered from two rainfall stations: JPS Wilayah and Leboh Pasar. For the rainfall event that occurred on 29 October 2001, the JPS Wilayah station recorded 89 mm in three hours while 125 mm in three hours was recorded at the Leboh Pasar station. For the event that occurred on 10 June 2003 the recorded

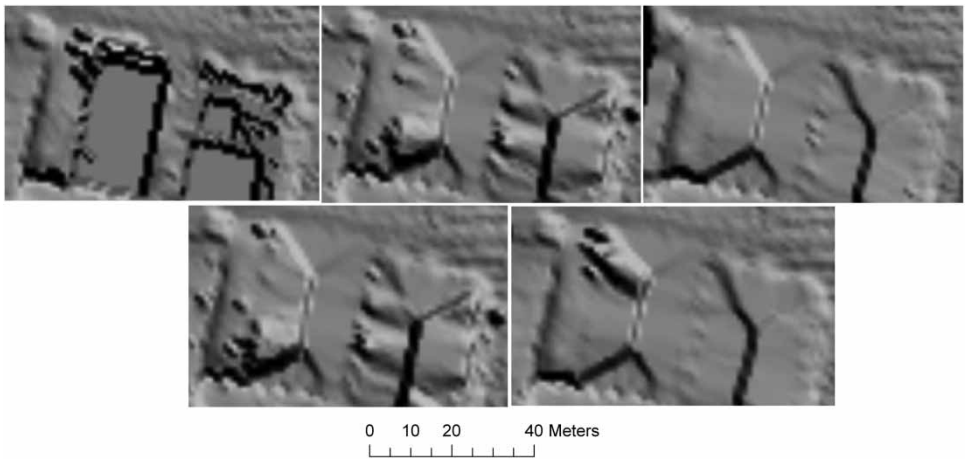

Figure 8 | Top: DTMs from MPMA, Morph and Poly. Bottom: DTMs from Morph2D and ATIN.

Table 2 | Adjustment values for factors that affect the roughness of floodplains (Arcement & Schneider 1984)

Flood-plain conditions	*n* value adjustment	
		Degree of irregularity (n_1)
Smooth	0.000	Compares to the smoothest, flattest flood-plain attainable in a given bed material
Minor	0.001–0.005	Flood plain slightly irregular in shape. A few rises and dips or sloughs may be more visible on the flood plain
Moderate	0.006–0.010	Have more rises and dips. Sloughs and hummocks may occur
Severe	0.011–0.020	Flood plain very irregular in shape. Many rises and dips or sloughs are visible. Irregular ground surfaces in pasture land and furrows perpendicular to the flow are also included
		Variation of flood-plain cross section (n_2)
Gradual	0.000	Not applicable
		Effect of obstruction (n_5)
Negligible	0.000–0.004	Few scattered obstructions, which include debris deposits, stumps, exposed roots, logs, piers, or isolated boulders, that occupy less than 5% of the cross-sectional area
Minor	0.040–0.050	Obstructions occupy less than 15% of the cross-sectional area
Appreciable	0.020–0.030	Obstructions occupy from 15% to 50% of the cross-sectional area
		Amount of vegetation (n_4)
Small	0.001–0.010	Dense growths of flexible turf grass, such as Bermuda, or weeds growing where the average depth of flow is at least two times the height of the vegetation; supple tree seedlings such as willow, cottonwood, arrow-weed, or salt cedar growing where the average depth of flow is at least three times the height of the vegetation
Medium	0.010–0.025	Turf grass growing where the average depth of flow is from one to two times the height of the vegetation; moderately dense steamy grass, weeds, or tree seedlings growing where the average depth of flow is from two to three times the height of the vegetation; brushy, moderately dense vegetation, similar to 1-to-2-year-old willow trees in the dormant season
Large	0.025–0.050	Turf grass growing where the average depth of flow is about equal to the height of the vegetation; 8-to-10-year-old willow or cottonwood trees intergrow with some weeds and brush (none of the vegetation in foliage) where the hydraulic radius exceeds 0.607 m or mature row crops such as small vegetables, or mature field crops where depth flow is at least twice the height of the vegetation
Very large	0.050–0.100	Turf grass growing where the average depth of flow is less than half the height of the vegetation; or moderate to dense brush, or heavy stand of timber with few down trees and little undergrowth where depth of flow is below branches, or mature field crops where depth of flow is less than the height of the vegetation
Extreme	0.100–0.200	Dense bushy willow, mesquite, and salt cedar (all vegetation in full foliage), or heavy stand of timber, few down trees, depth of reaching branches
		Degree of meander (m)
	1.0	Not applicable

rainfall at Station JPS Wilayah was 86 mm in four hours while the Leboh Ampang station recorded 125 mm in four hours. The data from both stations were used in model simulations in order to reflect the spatial variability.

The drainage channel network and the river were modelled with 1D model (MIKE 11). The calculated subcatchment discharges are introduced as lateral or concentrated inflows into the branches of the 1D model network. The hydrographs generated for each subcatchment were calculated using the NAM and nonlinear reservoir method. The floodplain flows were modelled with the 2D model (MIKE 21). The DTM along the channel network, providing the interface between the coupled 1D–2D models, was set to the bank-full level of the 1D model.

Upstream and downstream boundary conditions of the river model were derived from the results of the previously modelled Klang River model and introduced as inflows (upstream) and water level (downstream) into the model used in the present work. The flood extent shown in Figure 9 is due to the combined effects of river-related overbank discharges as well as discharges from the inland drainage system.

As shown in Figure 9, for an event that occurred on 29 October 2001, it can be observed that there are significant differences between computed and recorded data. For the Morph, Morph2D, Polynomial and Adaptive TIN filtering algorithms, the related 2D models showed a reasonable prediction of flood depths. This can be attributed to the difference in features filtered by the different algorithms and also the lack of capability in presenting buildings with a basement. The effect of floodwater entering and ponding the basement of the building first before continuing to flow into the surrounding area is obviously a critical aspect and the models which do not have such a representation are unlikely to produce fruitful results. It is because of this and other reasons that the results from MPMA appear to be closer to the measurements. The model results of flood depths are shown in Table 3.

Table 4 shows the summary of modelled and measured flood depths for the flood event that occurred on 10 June 2003. From this table it can be observed that the model

Table 3 | Summary of modelled and measured flood depths for 29 October 2001 rainfall event

Location Flood depth (m)	Dataran Merdeka (1)	Leboh Ampang (2)	Tun Perak (3)	Jalan Melaka (4)	Kg. Pantai Halt (5)
MEASURED	0.370	1.870	0.870	1.370	0.540
1D/2D model with MPMA DTM	0.410	1.656	0.745	1.238	0.949
1D/2D model with POLY DTM	0.599	1.303	0.599	1.702	1.540
1D/2D model with MORPH DTM	0.532	1.240	0.361	1.617	1.380
1D/2D model with MORPH2D DTM	1.207	0.825	0.353	2.134	1.350
1D/2D model with ATIN DTM	1.165	1.033	0.403	1.135	1.186

Numbers in brackets refer to location identified in Figure 9.

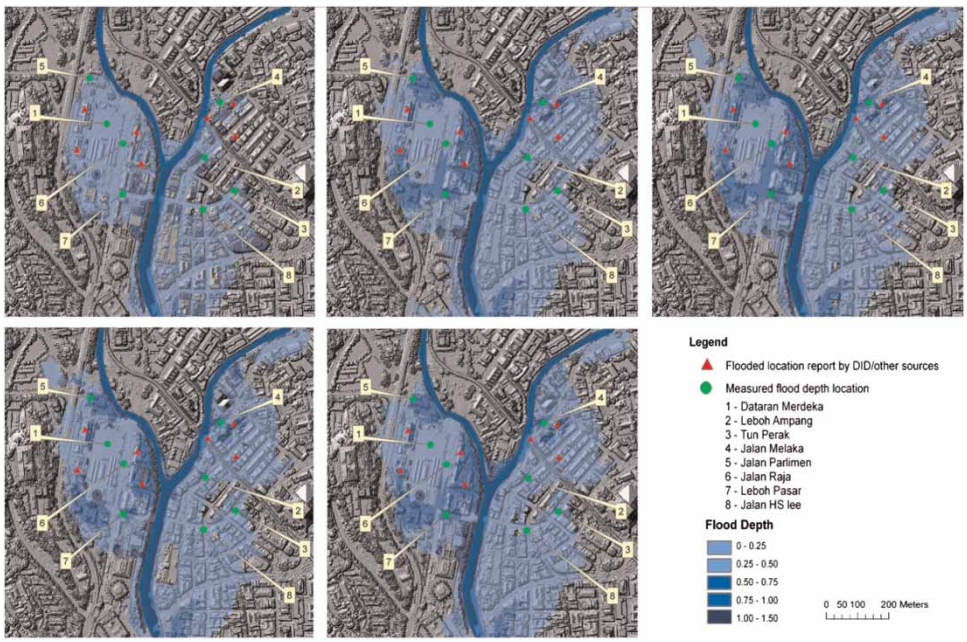

Figure 9 | Modelled and observed flood locations for 10 June 2003 rainfall event. Top: predictions by models with DTMs generated from MPMA, Morph and Morph2D algorithms. Bottom: predictions by models with DTMs generated from Poly and ATIN algorithms. Observed locations are represented with triangles and circles.

Table 4 | Summary of modelled and measured flood depths (in metres) for 10 June 2003 rainfall event at different locations

	Dataran Merdeka (1)	Leboh Ampang (2)	Tun Perak (3)	Jalan Melaka (4)	Jalan Parlimen (5)	Jalan Raja (6)	Leboh Pasar (7)	Jalan HS Lee (8)
MEASURED	0.500	1.200	1.000	1.300	0.500	1.000	0.650	1.000
1D/2D model with MPMA DTM	0.923	1.192	0.964	1.621	0.855	0.877	0.748	0.996
1D/2D model with POLY DTM	1.250	1.219	1.067	1.822	1.240	1.588	1.071	1.005
1D/2D model with MORPH DTM	1.471	1.254	1.180	1.910	1.395	1.787	1.319	0.911
1D/2D model with MORPH2D DTM	1.469	1.321	1.195	1.995	1.402	1.859	1.363	1.061
1D/2D model with ATIN DTM	1.392	1.210	0.885	1.792	1.153	1.666	1.260	0.885

Numbers in brackets refer to location identified in Figure 9.

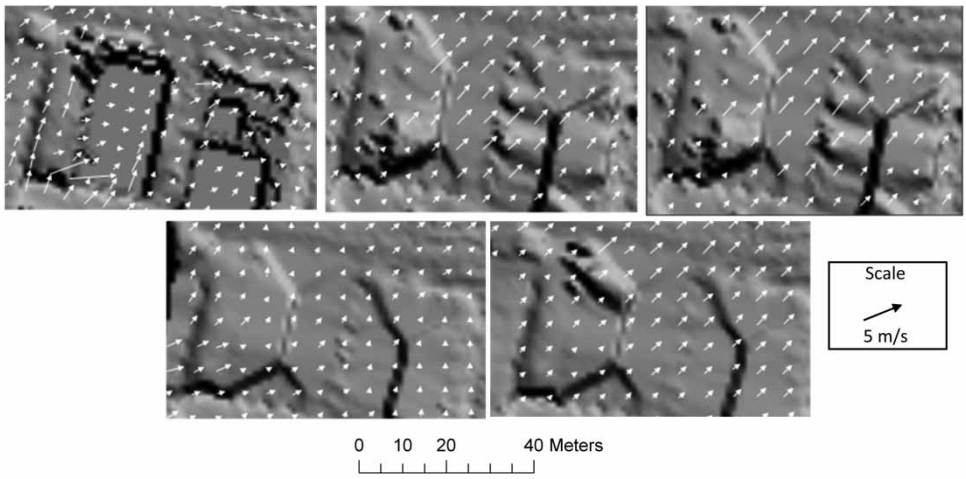

Figure 10 | Comparison of velocity vectors. Top row shows modelled velocity vectors and DTMs generated from MPMA, Morph and Poly. Bottom: row shows modelled velocity vectors and DTMs generated from Morph2D and ATIN.

which uses the DTM built from the MPMA algorithm gives the closest result to the measurements. This can be explained by the fact that in MPMA DTM the buildings are more adequately represented. On average, the difference in flood depths of 39% was observed between a model that uses a DTM modified by the MPMA algorithm and the predictions of other models (Tables 3 and 4).

For the analysis of flood extents in addition to the measurements taken at several locations by DID local observations were also sourced from newspapers such as Utusan Malaysia, The Sun, New Strait Times, The Star, and Harian Metro and Berita Harian. These data were introduced into GIS layers and then overlaid with the model results for comparison purposes. Figure 9 illustrates flood extents produced by five 1D/2D models against local observations. From Figure 9 it can be observed that flood extents obtained from all models are in a reasonably good agreement with the measurement but the extent from Morph, ATIN, Morph2D and Poly appears to be larger from what was recorded. Again, the model results based on MPMA DTM were found to be more close to local observations than other model results.

From the analysis of computed flood velocities it can be observed that the results from 1D/2D model that uses the DTM from the MPMA algorithm are closer to reality as

they better represent the physics of the phenomena; see Figure 10. This is more or less a consequence of the ability of MPMA to recreate the basement condition in the DTM where the flood water is allowed to inundate the basement area first before it floods the surrounding area. Not only that, the assigned Manning value of 20 ($n = 0.05$) for passage buildings produces a flow that more closely represents the real phenomena. From the overall results it can be concluded that models with different DTMs can lead to significantly different flood predictions. The difference in results suggests the importance of a careful consideration of building objects for urban floodplain modelling.

CONCLUSION

This paper presents the augmentation of an existing progressive morphological filtering algorithm for processing raw LiDAR data to support a 1D/2D urban flood modelling framework. Several LiDAR filtering algorithms were compared and it was found that none of them in their present form is fully suitable to support urban flood modelling work. As a result, the existing PMA algorithm was modified to incorporate *buildings with basement*, *passage buildings* and *solid buildings*. The new assumptions for closed polygon buildings in vector form have been introduced in order to identify different building features from point cloud data. The concept of downward expansion in representing building basements has also been introduced. For those buildings that act as passage buildings the use of different roughness parameter values was implemented.

The value of the modified algorithms was demonstrated on a case study from Kuala Lumpur Malaysia where the model results were analysed and compared against recorded data in terms of flood depths, flood extents and flood velocities. The overall analysis of model results suggest that incorporation of building basements within the DTM can lead to a significant difference in the model results with a tendency towards overestimation for those models which do not incorporate such a feature. The difference in flood depths with an average of 39% was observed between a model that uses a DTM modified by the MPMA algorithm and the predictions of other models.

REFERENCES

Abbott, M. B. & Rasmussen, C. H. 1977 On the numerical modelling of rapid expansions and contractions in models that are two-dimensional in plan. In *IAHR Conference, Baden-Baden, 14 August 1977*. Plenum Publishing Corporation, Baden-Baden, Germany.

Abbott, M. B. & Vojinovic, Z. 2009 Applications of numerical modelling in hydroinformatics. *J. Hydroinf.* **11** (3–4), 308–319.

Adelson, E. H., Anderson, C. H., Bergen, J. R., Burt, P. J. & Ogden, J. M. 1984 Pyramid methods in image processing. *RCA Engineer* **29** (6), 33–41.

Arcement, G. J. & Schneider, V. R. 1984 *Guide for Selecting Manning's Roughness Coefficients for Natural Channels and Floodplains.* Report FHWA-TS 84, 204, US Department of Transportation, Federal Highway Administration.

Axelsson, P. 1999 Processing of laser scanner data – algorithms and applications, *ISPRS J. Photogramm. Remote Sens.* **54** (2–3), 138–147.

Becker, B. & Schüttrumpf, H. 2010 An OpenMI module for the groundwater flow simulation programme Feflow. *J. Hydroinf.* **13** (1), 1–12.

Chen, A. S., Hsu, M. H., Teng, W. H., Huang, C. J., Yeh, S. H. & Lien, W. Y. 2006 Establishing the database of inundation potential in Taiwan. *Natl Hazards* **37** (1–2), 191–207.

Cowan, W. L. 1956 Estimating hydraulic roughness coefficients. *Agric. Engng* **37** (7), 473–475.

Dawson, R. J., Speight, L., Hall, J. W., Djordjevic, S., Savic, D. & Leandro, J. 2008 Attribution of flood risk in urban areas. *J. Hydroinf.* **10** (4), 275–288.

DHI (Danish Hydraulics Institute) 2004 *Klang River basin Environmental Improvement and Flood Mitigation Project (ADB): Stormwater Management and Road Tunnel (SMART), Final Report.* Department of Irrigation and Drainage, Malaysia.

Djordjević, S., Prodanović, D., Maksimović, C., Ivetić, M. & Savić, D. A. 2005 SIPSON – Simulation of interaction between pipe flow and surface overland flow in networks. *Water Sci. Technol.* **52** (5), 275–283.

Elmqvist, M. 2002 Ground surface estimation from airborne laser scanner data using active shape models. *IAPRS* **XXXIV**, 114–118.

Hsu, M. H., Chen, S. H. & Chang, T. J. 2000 Inundation simulation for urban drainage basin with storm sewer, *Syst. J. Hydrol.* **234** (1–2), 21–37.

Hunter, N. M., Bates, P. D., Neelz, S., Pender, G., Villanueva, I., Wright, N. G., Liang, D., Falconer, R. A., Lin, B., Waller, S., Crossley, A. J. & Masoc, D. C. 2008 Benchmarking 2D hydraulic models for urban flooding. *Water Manag.* **161**, 13–30.

Hu, Y. 2003 *Automated Extraction of Digital Terrain Models, Roads and Buildings Using Airborne LiDAR Data*. PhD Thesis, University of Calgary, Canada.

Lamb, R., Crossley, A. & Waller, S. 2009. A fast two-dimensional floodplain inundation model. *Proc. Inst. Civil Eng. – Water Manag.* **162** (6), 363–370.

Mark, O., Weesakul, S., Apirumanekul, C., Aroonnet, S. B. & Djordjevic, S. 2004 Potential and limitations of 1D modelling of urban flooding, *J. Hydrol.* **299** (3–4), 284–299.

Mynett, A. E. & Vojinovic, Z. 2009 Hydroinformatics in multi-colours – part red: urban flood and disaster management, *J. Hydroinf.* **11** (3–4), 166–180.

Neal, J. C., Fewtrell, T. J., Bates, P. D. & Wright, N. G. 2010 A comparison of three parallelization methods for 2D flood inundation models, *Environ. Modell. Softw.* **25** (4), 398–411.

Neal, J. C., Fewtrell, T. & Trigg, M. 2009 Parallelisation of storage cell flood models using OpenMP. *Environ. Modell. Softw.* **24** (7), 872–877.

Petersen, O., Rasmussen, E. B., Enggrob, H. & Rungø, M. 2007 *Modelling of Flood Events Using Dynamically Linked 1D and 2D Models.* Florida Floodplain Managers Association. Available from: http://www.ffma.net/pdf/mfloodPaper.pdf (accessed October 2007).

Pfeifer, N. & Stadler, P. 2001 Derivation of digital terrain models in the SCOP environment. In *Proceedings of the OEEPE Workshop on Airborne Laserscanning and Interferometric SAR for Detailed Digital Elevation Models, 1–3 March 2001, Stockholm, Sweden.*

Price, R. & Vojinovic, Z. 2011 *Urban Hydroinformatics*. IWA Publishing, London.

Roncat, A., Dorninger, P., Molnár, G., Székely, B., Zámolyi, A., Melzer, T., Pfeifer, N. & Drexel, P. 2010 Influences of the acquisition geometry of different Lidar techniques in high-resolution outlining of microtopographic Landforms. In *Fachtagung Computerorientierte Geologie – COGeo 2010, 11 June 2010, Salzburg, Austria,* 17pp.

Schumann, G., Matgen, P., Cutler, M. E. J., Black, A., Hoffman, L. & Pfister, L. 2007 Comparison of remotely sensed water stages from LiDAR, topographic contours and SRTM. *ISPRS J. Photogramm. Remote Sens.* **63** (3), 283–296.

Seyoum, S. D., Vojinovic, Z. & Price, R. 2010 Urban pluvial flood modeling: development and application. In *Proceedings of the 9th International Conference on Hydroinformatics, HIC 2010, September 7–11, 2010, Tianjin, China*.

Sithole, G. & Vosselman, G. 2001 Filtering of laser altimetry data using a slope adaptive filter. *In IAPRS*, Vol. XXXIV, 3/W4, Annapolis, MD, USA.

Sithole, G. & Vosselman, G. 2004 Experimental comparison of filter algorithm for bare earth extraction from airborne laser scanning point clouds. *ISPRS J. Photogramm. Remote Sens.* **56**, 85–101.

Tsubaki, R & Fujita, I. 2010 Unstructured grid generation using LiDAR data for urban flood inundation modeling. *Hydrol. Process.* **24**, 1404–1420.

Vojinovic, Z. & Abbott, M. B. 2011 *Urban Hydroinformatics: The Sociotechnical Dimensions of Urban Flood Risk Management*. IWA Publishing, London.

Vojinovic, Z., Bonillo, B., Chitranjan, K. & Price, R. 2006 Modelling flow transitions at street junctions with 1D and 2D models. In *Proceedings of the 7th International Conference on Hydroinformatics, September 2006, Nice, France*.

Vojinovic, Z., Salum, M. H., Seyoum, S. D., Mwalwaka, J. M., Price, R. K. & Abdullah, A. F. 2010a Modelling urban floodplain inundation with different spatial resolution and model parameterisation. In *Proceedings of the 9th International Conference on Hydroinformatics, HIC 2010, September 7–11, 2010, Tianjin, China*.

Vojinovic, Z., Seyoum, S. D., Mwalwaka, J. M. & Price, R. K. 2010b Effects of model schematization, geometry and parameter values on urban flood modelling. *Water Sci. Technol.* (in press).

Vojinovic, Z. & Tutulic, D. 2009 On the use of 1D and coupled 1D–2D modelling approaches for assessment of flood damage in urban areas. *Urban Water J.* **6**, 183–199.

Vosselman, G. 2000 Slope based filtering of laser altimetry data. *Int. Arch. Photogramm. Remote Sens. Spatial Inf. Sci.* **33** (B3/2), 935–942.

Wack, R. & Wimmer, A. 2002 Digital terrain models from airborne laser scanner data – a grid based approach. *IAPRS* **XXXIV** pp. 293–296. In *ISPRS Commission III, Symposium, September 9–13, 2002, Graz, Austria*.

Zhang, K. Q., Chen, S. C., Whitman, D., Shyu, M. L., Yan, J. H. & Zhang, C. C. 2003 A progressive morphological filter for removing nonground measurements from airborne LiDAR data. *IEEE Trans. Geosci. Remote Sens.* **41** (4), 872–882.

Zhang, K. & Cui, Z. 2007 *Airborne LiDAR Data Processing and Analysis Tools ALDPAT 1.0 Software Manual.* National Center for Airborne Laser Mapping, Florida International University, Miami.

Zhang, K. & Whitman, D. 2005 Comparison of three algorithms for filtering airborne LiDAR data. *Photogramm. Engng Remote Sens.* **71**, 313–324.

First received 7 July 2010; accepted in revised form 8 November 2010. Available online 18 April 2011